Available online at www.sciencedirect.com
SCIENCE DIRECT®

Polymer 47 (2006) 4203–4209

polymer

www.elsevier.com/locate/polymer

Development of techniques to compare mechanical properties of reversible hydrogels with spherical, square columnar and ocular lens geometry

N. Ravi [a,b,c,*], K.T. Wan [d], K. Swindle [a,b], P.D. Hamilton [a], G. Duan [d]

[a] *Department of Veterans Affairs, St Louis, MO, USA*
[b] *Department of Chemical Engineering, St Louis, MO, USA*
[c] *Department of Ophthalmology and Visual Sciences, Washington University, St Louis, MO, USA*
[d] *Department of Mechanical Engineering, University of Missouri-Rolla, Rolla, MO, USA*

Abstract

We have developed a new experimental technique for determining the elastic modulus of the ocular lens by using hydrogel phantoms. We successfully prepared disulfide-reversible polyacrylamide hydrogels in the forms of a square column, a sphere, and a lens. The M_n (number average molecular weight) of the reduced copolymer ranged from 696,800 to 870,900 Da. The physical and swelling properties of the gels were independent of shape. The M_c (molecular weight between cross-links) ranged from 1776 to 1887 compared with the theoretical M_c of 1638 Da. The gels exhibited non-linear rubber elasticity, but at low strains the elastic moduli (E) were 4680 ± 150, 5010 ± 280, and 4870 ± 220 Pa for the square column, sphere, and lens, respectively. The shear modulus (G) was 1531 ± 70 Pa with an E/G ratio of approximately 3:1, indicating an incompressible gel at low strains. At high strains ($\sim 15\%$) the Mooney–Rivlin plot was linear and the magnitude of $2C_1$ was 1515 Pa, which was comparable to the shear modulus of the gels. Finally, the Tatara mechanical model for large deformation of rubber spheres was successfully applied to extract the elastic modulus of the lens. The modulus of the lens obtained with this technique was consistent with the moduli for the square column and sphere. The new technique will be used to determine the mechanical properties of the ocular lens.

Keywords: Hydrogel; Lens; Biomechanics

1. Introduction

A hydrogel is a polymer network swollen in water. The network may be prepared from synthetic or natural polymer chains through covalent or physical cross-links. Its ability to absorb a large amount of water is the most significant property because it has a profound effect on permeability, mechanical properties, surface characteristics, and biocompatibility. The hydrogel, depending on its composition and structure, is capable of retaining water, hydrocarbons, solutes, and gas bubbles, and can respond to the local environment. Its sensitivity to local environments not only has been advantageously applied in biology and medicine, but is also of fundamental scientific importance, which has all been recently reviewed [1–5].

For decades scientists have devoted their attention to the investigation of the biomechanics of tissues. Finding three-dimensional (3D) constitutive equations relating stress to strain for tissue is not simple. Biological tissues usually have complex, non-homogenous, anisotropic internal architecture. This diverse architecture displays elastic, plastic, viscoelastic, poroelastic, or poroviscoelastic properties [6,7]. In spite of this complexity, much progress has been achieved by performing various simple tests, particularly, in shear elongation or compression, and developing more complex models and 3D constitutive equations [8].

Our interest in water-swollen polymer networks stems from their ability to serve as synthetic substitutes or mechanical probes in the investigation of biomechanics of the ocular lens [9,10]. Age-related changes in the viscoelastic properties of the lens have been implicated in the pathophysiology of presbyopia, a clinical condition in which even a normal eye is not able to focus at arm's length. The use of bifocals is necessary. The salient feature of the lens is that it is a biconvex aspherical tissue with an elastic membrane enclosing a well-organized collection of lens epithelial cells that are

---

* Corresponding author. Address: Department of Ophthalmology and Visual Science, Washington University School of Medicine, Campus Box 8096, 660 South Euclid, St Louis, MO 63110, USA. Tel.: +1 314 747 4458; fax: +1 314 289 7034.

E-mail addresses: nathan.ravi@med.va.gov (N. Ravi), ravi@vision.wustl.edu (N. Ravi).

0032-3861/$ - see front matter © 2006 Elsevier Ltd. All rights reserved.
doi:10.1016/j.polymer.2006.02.029

differentiated in close-packed hexagonal elongated fibers. The fibers are generally devoid of organelles, and the cytoplasm consists primarily of a concentrated solution of proteins referred to as the lens crystalline proteins. Cutting the lens into a standard geometrical form destroys the delicate architecture that gives rise to its mechanical properties, thus confounding the experimental values. In spite of these challenges, certain general mechanical properties about the lens are known. For instance, the collagenous capsular membrane behaves as a non-linear elastic material [11–14], whereas the delicate collection of organized lens fibers exhibits solid-like viscoelastic properties with a modulus ranging from 0.75 to 10.9 kPa [15–18], depending on the age, the species, and the technique used. Our ultimate goal is to develop a robust axisymmetric finite-element model for investigating the biomechanics of the lens. The delicate aspherical biconvex surface renders it difficult to determine the elastic properties by a standard parallel-plate compression method because of the changing plate–lens surface contact area. To obtain more insight into the mechanical properties of the lens, it was necessary to determine how the modulus of a spherical biconvex soft material could be extracted from the data of applied force, sample dimensions, and plate–plate separation.

To answer this question, we turned to polymeric phantoms that can be molded into different shapes and whose physical and mechanical properties can be determined by expounding on known theoretical foundations. Polymer hydrogel phantoms were prepared by solution copolymerization of acrylamide with concurrent cross-linking with a disulfide bisacrylate. Implicit in our methodology is the assumption that if one uses the same composition of polymerizing solution and reaction conditions in molds of differing shapes of approximate similar sizes, then the moduli of the final gel must be nearly identical. From previous work in our laboratory, we had identified a hydrophobic acrylamide copolymer that did not swell significantly and yet was soft [19]. Additionally, the use of the easily cleavable disulfide –S–S– linkage in the cross-linker structure, with appropriate reducing agents, enables complete liquefaction of the gel into a water-soluble thiol-containing copolymer. This makes it possible to measure M_n (number average molecular weight) and the subsequent determination of M_c (molecular weight between cross-links) through an assay of the amount of free thiol group per chain. We used and extended theories of polymer network elasticity and theories of Hertz [20] and Tatara [21,22] that were initially developed for mechanical modeling of rubber spheres between parallel plates, to biconvex spherical gels in compression.

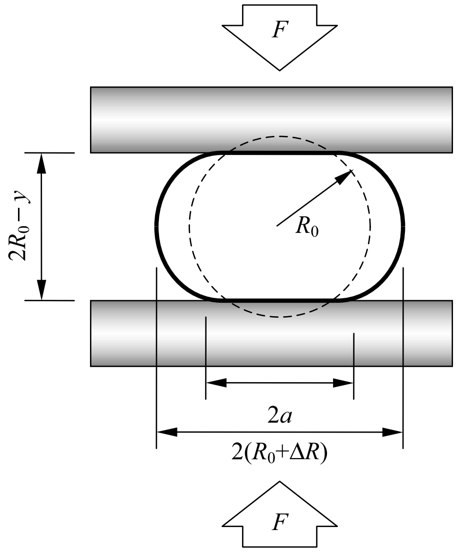

Fig. 1. Schematic of parallel-plate compression and variables used in the mechanical model.

1.1. Theory

For a column with height, ℓ; a uniform square cross-section with side, s; an area, $A=s^2$; and an external load, F, the uniform mechanical stress, σ, is thus given by

$$\sigma=\frac{F}{A}=\underbrace{E}_{\text{Materials properties}}\times\underbrace{\frac{1}{\ell}}_{\text{Geometrical parameter}}\times\underbrace{y}_{\text{Mechanical response}} \tag{1}$$

where y is the decrease in column height due to compression. Once the mechanical response, $F(y)$, is experimentally measured, the value of E can be determined.

The classic Hertz [20] model allows for the deformation of a spherical sample being squashed between two parallel plates to be fully described within the limits of certain assumptions. For instance, the radius of contact, a, is small compared with the radius of the undeformed sphere, R_0; the deformation is small and within linear elastic limits; and there is an absence of adhesion and friction resulting in the transfer of only normal stresses between the contacting surfaces. Upon application of an external force, F, the sphere of elastic modulus, E, and Poisson ratio, ν, deforms according to

$$F=\frac{\sqrt{2}}{3}\left(\frac{E}{1-\nu^2}\right)R_0^{1/2}y^{3/2} \tag{2}$$

where y characterizes the approach of the parallel plates toward each other during compression. Thus, the elastic force is proportional to 3/2 power of approach, and the gradient of $F(y)$ in a log–log plot is proportional to E. For large deformation, as in the current studies, incorporation of the non-linear rubber elasticity model becomes necessary [23,24]. Recently, Tatara [21,22,25] developed a general theory for the compressive deformation for a homogenous non-adhesive rubber sphere under large deformation ($>15\%$ strain) with non-linear elastic behavior. Here, the model derived by Tatara [21,22,25] was adopted. Fig. 1 shows a sphere with an original radius, R_0, being compressed by an external load, F. At equilibrium, the distance of approach (relative movement of the two plates) becomes y, the equatorial radius increases from R_0 to $R=(R_0+\Delta R)$ with ΔR the lateral extension of the equatorial radius, and the sphere–substrate point contact extends to a radius of a.

The constitutive relations are listed as follows

$$y = \underbrace{\left(\frac{1}{\pi E R_0}\right)\left[\frac{3\pi(1-\nu^2)}{4\alpha}\right]F.}_{\text{Hertz model for small deformation}} - \underbrace{\left(\frac{2}{\pi E R_0}\right)\left[\frac{1+\nu}{(4+\alpha^2)^{3/2}} + \frac{1-\nu^2}{2(4+\alpha^2)^{1/2}}\right]F}_{\text{Additional term due to large deformation}} \quad (3)$$

$$\Delta R = \frac{1+\nu}{\pi E R_0}\left[\frac{1}{2\sqrt{2}} - (1-2\nu)\left(1-\frac{1}{\sqrt{2}}\right)\right]F \quad (4)$$

$$a^3 = \frac{3(1-\nu^2)R_0 F}{4E} \quad (5)$$

with $\alpha = a/R_0$. By combining Eqs. (3)–(5), the ‘apparent mechanical stress’ is given by:

$$\sigma = \frac{F}{\pi R_0^2} = \underbrace{E}_{\text{Materials properties}} \times \underbrace{\frac{2}{R_0}\left[\frac{3\pi(1-\nu^2)}{8\alpha} - \frac{1+\nu}{(4+\alpha^2)^{3/2}} - \frac{1-\nu^2}{2(4+\alpha^2)^{1/2}}\right]^{-1}}_{\text{Geometrical parameter}} \times \underbrace{y}_{\text{Mechanical response}} \quad (6)$$

Note the similarity between Eqs. (1) and (6). In Eq. (6), σ is not the rigorous engineering stress because the contact area expands (and α) at an increasing F. Eq. (6) can also be rewritten with α replaced by ΔR with Eq. (5). The term in the square bracket denotes the changing geometry due to the increasing contact circles, or the deviation of the shape from a square one. When the constitutive relation, $F(y,a,\Delta R)$, is determined experimentally with simultaneous measurements of F, y, a and ΔR, the value of E can be deduced. It is, however, practically cumbersome to measure a at a designated F because of the extra force on the sample due to intrinsic weight of the sample and the possible long-range surface forces at the sample–substrate interface. Therefore, for simplicity only Eq. (4) will be adopted in the following data analysis, despite the shortcomings in the determination of F. Nonetheless, the equation possesses only two variables, namely, F and ΔR, which reduce the degree of uncertainty. For an incompressible sphere, $\nu = 0.50$ and (4) reduces to:

$$\Delta R = 0.16881\frac{F}{E R_0} \quad (7)$$

A linear relation $\Delta R(F)$ is expected of the experiments, and E can be deduced accordingly.

The model lens geometry comprises a hemispherical bottom half with radius, R_0, and a spherical cap with a minor axis smaller than R_0. The two halves are joined at an equator of radius R_0. The solid model for such a convoluted geometry is mathematically involved and currently unavailable in the literature. Consequently, for simplicity, the stress fields developed in the two halves are assumed to be independent of each other. This assumption is applicable if the equatorial plane does not shift toward either pole upon loading. The experimental results validate this assumption. Eq. (7) will be used to determine E.

2. Experimental

The monomers and cross-linking agents used in this research were purchased at the highest purity available from Aldrich or Sigma Chemical Co. (St Louis, Mo) and were used without further purification. All solvents and other reagents used were analytical grade.

2.1. Preparation of poly(AAm-co-BAC-co-NPA) hydrogel

Acrylamide (AAm), the cross-linker bisacryloylcystamine (BAC), and *N*-phenylacrylamide (NPA) (Fig. 2) were copolymerized at acrylic mole ratios of 91/4.5/4.5 at 7.5% (w/w) final monomer concentration in 25% ethanol (25:75 = ethanol:water v/v). Polymerization was carried out by free radical polymerization with *N*,*N*,*N*′,*N*′-tetramethylethylenediamine (TEMED) and ammonium persulfate (APS). The preparation of the hydrogel has been previously reported [19]. The polymer obtained was labeled as $AB_{(4.5)}$–$N_{(4.5)}$. After mixing, the solutions were pipetted into a standard square Teflon mold, plus two acrylic molds, one spherical and one lens shaped, and maintained for 16 h at room temperature for complete gelation and cross-linking copolymerization. Gels were then placed in distilled water and washed with changes twice a day for 3 days to wash out most of the extractable materials and allow them to reach equilibrium volume.

2.2. Gel characterization

The density of the gel was determined with an analytical balance by means of ASTM standard for the measurement of density by buoyancy method, using the following Eq. (8):

$$\rho = \frac{\text{Weight}_{\text{in air}} \times \rho_{\text{liquid}}}{\text{Weight}_{\text{in air}} - \text{Weight}_{\text{in liquid}}} \quad (8)$$

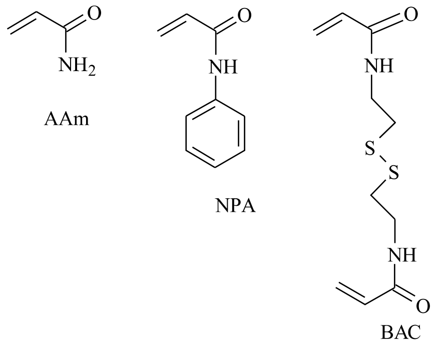

Fig. 2. Monomers used in preparation of poly(Aam-co-BAC-co-NPA) hydrogel.

Measurements were carried out on five samples, and the average and standard deviation were determined.

Equilibrium swelling was determined by dividing the swollen volume of the gel by its initial volume on removal from the mold at the condition at which it was formed.

Mechanical properties of the gels were determined with the Perkin–Elmer DMA 7e dynamic mechanical analyzer (Perkin–Elmer Corp., Norwalk, Conn.). After the probe was zeroed, the sample was placed in water maintained at 22 °C, and the top plate was lowered gently. Care was taken to immerse the hydrogel in water without any water collecting on the top plate. The water level was also adjusted and maintained to just touching the moveable plate so that buoyancy force due to plate submersion could be safely ignored. The sample was allowed to equilibrate at this condition, and then force was applied from 0 to 100 mN at 5 mN/min. Previously, the moduli determined at various stress rates were found to be independent of rates below 5 mN/min, but increased significantly at higher rates. Thus this condition was adopted. Photographs were taken at 2-min intervals with a digital camera (Minolta, Dimage Z2) equipped with a 10× optical zoom lens using manual focus with automatic shutter and depth of field settings. Measurements taken from the images were made against the 20 mm circular glass coverslip which was placed underneath the gels and was present in all conditions. The instrument compliance was less than 0.001% of the sample's compliance, and hence no correction was required. For the square column gels, the slope of the stress–strain plot at low strains ($<5\%$) gave the elastic modulus (E). The shear modulus, G, for low strains, was obtained from the slope of stress (σ) versus $\lambda-\lambda^{-2}$, where λ is the deformation ratio. For strains higher than 5%, G was verified with the Mooney–Rivlin equation:

$$\sigma = 2C_1(\lambda-\lambda^{-2}) + 2C_2(1-\lambda^{-3}) \tag{9}$$

In Eq. (9), $2C_1$ is equal to G in the classical rubber elasticity theory. For the spherical and lens-shaped gels, parameters from the digital pictures as well as the force applied from the DMA were used in Eq. (7) to estimate the Young's modulus.

Table 1
Network properties of polyacrylamide gels

Sample	Density (g/cm^3)	Q	M_n (Da)	M_c (Da)	PD	η (dL/g)
Square column	1.012±0.001	1.53±0.002	708,500	1776	1.335	0.954
Sphere	1.014±0.001	1.54±0.01	870,900	1859	1.169	1.06
Lens	1.014±0.002	1.57±0.02	696,800	1887	1.315	0.976

Table 2
Mechanical properties of hydrogels determined from DMA force data, with digital imaging or DMA and caliper measurements of the gel size

Sample	Elastic modulus from digital imaging size measurements (Pa)	Elastic modulus from DMA (Pa)	Shear modulus from DMA (Pa)
Square column	4860±150	4621±171	1531±70
Sphere	5010±280		
Lens	4870±220		

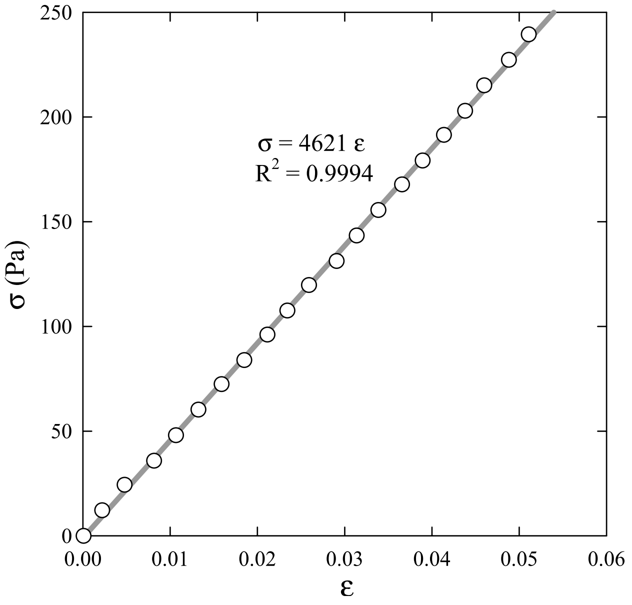

Fig. 3. Stress-strain plot for square column gel at low strain ($<5\%$) performed at 5 mN/min.

2.3. Reductive dissolution of polyacrylamide gels by dithiothreitol

Typically, the liquefaction of crushed gels was achieved by the addition of dithiothreitol (DTT) at a 10:1 mole ratio of BAC used. Nitrogen was bubbled through the solution under stirring, and the reduction was carried out for 4 h at pH 7.0. After complete solubilization, the copolymer solution was acidified to pH 4 with 10% (v/v) HCl and precipitated in excess volume of acidified methanol (pH 4) under vigorous stirring. The

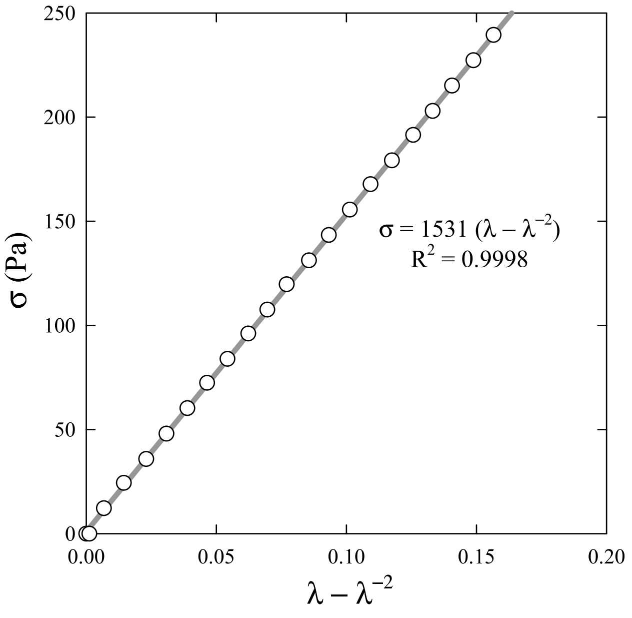

Fig. 4. Stress-strain plot for square column at all strains.

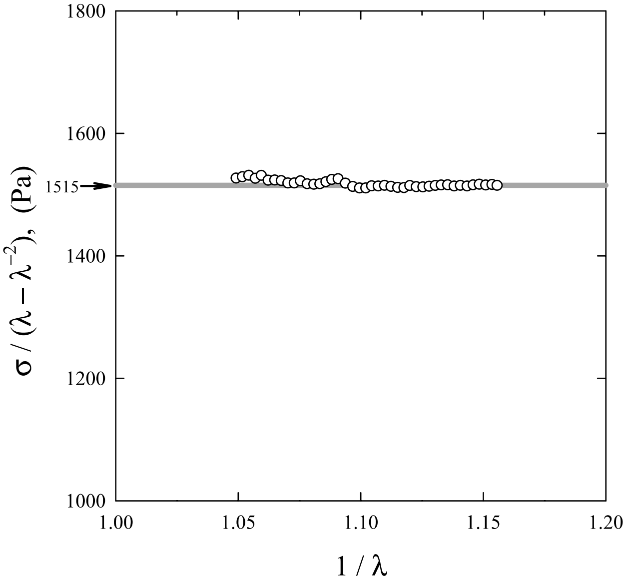

Fig. 5. Mooney-Rivlin plot for square column at large deformation (<15%).

precipitated copolymer was filtered, dried under vacuum, and stored under vacuum at all times.

The thiol (–SH) content present in the $AB_{4.5}$–$N_{4.5}$–SH copolymer was determined with Ellman's reagent [26]. Briefly, 20 μL of 0.5% (w/v) copolymer solution (pH 4, nitrogen bubbled) was added to a mixture of 50 μL of 0.01 M Ellman's reagent (in 0.1-M phosphate buffer, pH 8.0), 500 μL of 0.1-M phosphate buffer (pH 8), and 480 μL of distilled water. The absorbance (using Beckman DU54 spectrophotometer) of the resulting solution at 412 nm was obtained. The concentration of the –SH in the ABSH polymers was determined with the molar absorptivity of 13,600 $M^{-1}cm^{-1}$.

The molecular weight of the $AB_{(4.5)}$–$N_{(4.5)}$–SH copolymer was determined with an HPLC–GPC system equipped with three detectors (refractive index, light scattering, and viscosity; Viscotek, Houston, Tex.). The stationary phase consisted of a column of G4000PWXL (Tosoh Biosep, Montgomery Ville, Pa.), and the mobile phase was 20 mM Bis–Tris buffer (pH 6.0, 0.1% sodium azide). A polyethylene glycol standard (PolySciences, Warrington, Pa.) of molecular weight (M_w) 110,000 was used for calibration. Samples were prepared in water (pH 4, N_2 saturated) at a concentration of 0.5% (w/v). The M_c was directly determined from knowing the M_n, which was obtained from GPC and the average number of SH– groups in each polymer chain.

3. Results and discussion

The determination of the biomechanical characteristics of the lens is challenging because of its unique architecture. In spite of several innovative techniques, quantitative characterization of the viscoelastic properties of the lens is not available because of a lack of theoretical foundation on the effect of geometry on the mechanical response. This is our first paper, in a series of papers, in which we will systematically develop both the theoretical foundations and the experimental techniques for quantitatively describing the viscoelastic properties of the lens. This is a critical link in developing a robust finite element model to determine the cause of presbyopia and identify possible methods of treatment. We have extended the seminal work of Hertz [20] and Tatara [21,22,25] on the mechanical properties of rubber spheres at low and high deformations, respectively, to that of the lens.

Polyacrylamide gels were prepared in different shapes, including a lens. Reversible polyacrylamide gels were first reported for gel electrophoresis of proteins and DNA [27,28]. The advantage of using disulfides is that the gels can be subsequently dissolved with appropriate mild reducing agent to provide a facile method of recovering separated DNA and protein samples. The disulfide chemistry has also been used for entrapment of islet cells for refillable bioartificial pancreas [29]. Nanogels and proteo-mimetic polymers have also been prepared with this chemistry [30,31]. The presence of easily and quantitatively reducible disulfide linkage also provided an easy method for characterization of network properties. The degree of swelling of non-ionic polymer hydrogels is a function of the cross-link density, which is defined as the average molecular weight between cross-links (M_c). The classic equation of Flory–Rehner [32], which is based on rubber

(a) Sphere

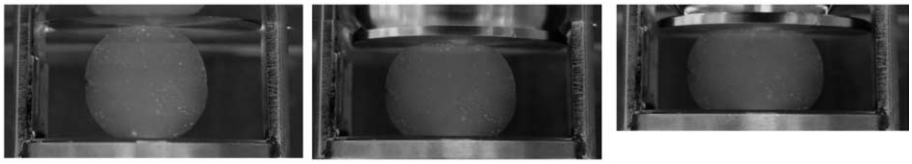

(a) Lens

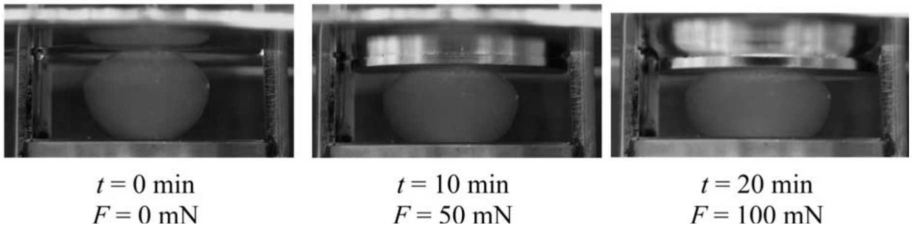

Fig. 6. Spherical- and lens-shaped gels shown between parallel plates during compression at $t = 0,10$, and 20 min.

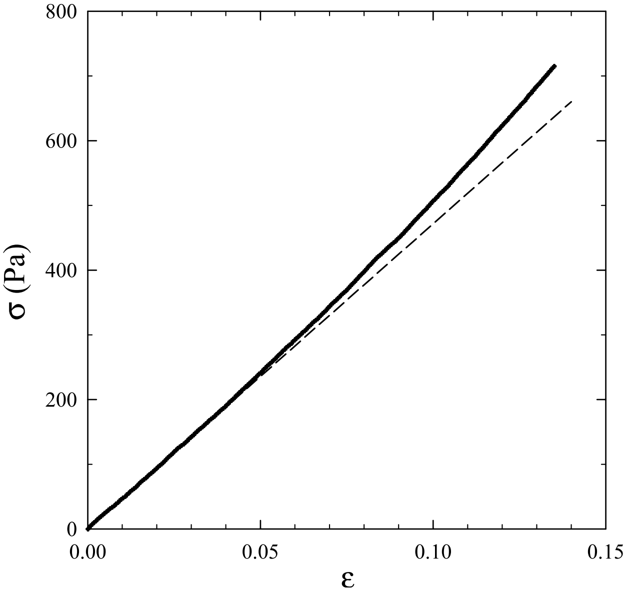

Fig. 7. Nonlinear characteristics of stress-strain plot for square column at large deformation performed at 5 m*N*/min.

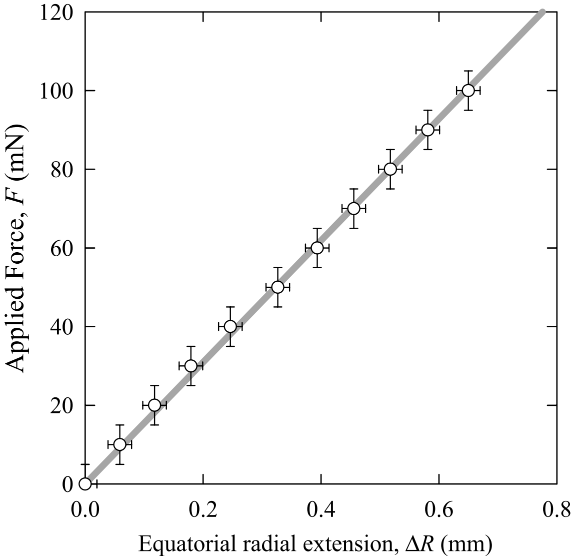

Fig. 8. Typical data of applied load as a function of radial expansion in the equatorial plan. Shown in a sphere with diameter $2R_0 = 10.19$ mm and elastic modulus $E_0 = 4800$ Pa.

elasticity, was first introduced to estimate M_c. The calculation of cross-links was based on assumptions of a network of chains exhibiting a Gaussian distribution to form a loosely cross-linked network. The equation is valid only for networks swollen from the solid state. Peppas and Merrill [33] have developed expressions for networks formed in solution. Their original formulation was for solution cross-linking of high molecular weight (Gaussian chain) polyvinylalcohol solution. Lee and Park [34] used reversible disulfide gels to confirm the Peppas and Merrill [33] equation formulated for calculating M_c from equilibrium swelling. Although similar calculations for non-Gaussian chains exist, the polar nature of water limits the use of such equations. To circumvent these limitations, we chose to work with disulfide-containing hydrogels so that the gels could be liquefied and the polymer could be characterized for M_n and the number of thiol groups. Table 1 summarizes the density, equilibrium swelling, M_n, M_c, polydispersity index, and intrinsic viscosity (η) of the hydrogels and the liquefied polymers. These values for all three gel shapes were reasonably close. M_n of the liquefied copolymers from GPC ranged from 697 to 871 K Da, and the polydispersity ranged from 1.17 to 1.34. The molecular weight is lower than that expected from theory on the basis of the molar ratio of the monomers to initiator. This might be due to the presence of ethanol in the cosolvent. Ethanol is known to significantly change the molecular kinetics, termination reaction, and network properties of similar systems [35]. If the copolymerization and cross-linking reaction were quantitative and the junctions were all tetra-functional, then the theoretical M_c, based on the stoichiometry of the monomers and cross-linkers, would be 1631 Da (the average molecular weight between cross-linking was taken to be 77.3 Da). The experimentally determined M_c ranged from 1779 to 1888 Da and was comparable to the expected value. All of these characteristics clearly indicate that our initial hypothesis that the network-relevant properties are independent of geometry is valid and that such a formulation can now be used to further the theoretical development for characterizing the mechanical properties of the lens.

Table 2 summarizes the experimental moduli of the hydrogels calculated from the digital imaging and DMA data. The DMA and caliper measurements of the gel dimensions could only be used to calculate the moduli of the rectangular columnar gels. Digital imaging was used to calculate the gel dimensions for the original and stressed square columns, spheres, and lenses. The elastic modulus for the square column was comparable for both calculation methods. Fig. 3 is the plot of the stress–strain data showing linearity with a slope equal to the elastic moduli at low strains. Similarly, Fig. 4 displays a plot of stress versus shear strain that is linear at low strains. As expected at larger strains, however, they exhibit non-linear elasticity and are, therefore, given in the form of the Mooney–Rivlin equation (Fig. 5). The fit is linear, and the intercept at $\lambda = 1.0$ is equal to $2C_1$, which is known to be of similar magnitude to the shear modulus. These moduli of the square column validate the experimental techniques. The mechanical property data also contain the values of the spherical and lenticular gels. Their moduli were expected to be the same within experimental limits, and they indeed were similar in magnitude. In Fig. 6 are examples of the digital pictures used for the moduli calculations, and Fig. 7 is a stress–strain plot for low and high strain values, which shows non-linear behavior at high strain. Fig. 8 shows the applied force as a function of radial expansion in the equatorial plane.

4. Conclusions

We have successfully prepared disulfide-reversible poly-acrylamide hydrogels in the forms of a square column, a sphere, and a lens. The M_n ranged from 696,800 to 870,900 Da. The physical and swelling properties of the gels were independent of shape. The M_c ranged from 1776 to 1887 Da compared with the theoretical M_c of 1638. The gels exhibited non-linear rubber elasticity, but at low strains the elastic moduli were 4680 ± 150, 5010 ± 280 and 4870 ± 220 Pa for the square column, sphere, and lens, respectively. The shear modulus was 1531 ± 70 Pa with a Poisson ratio of 0.5, indicating an incompressible gel at low strains. At high strains ($\sim 15\%$) the Mooney–Rivlin plot was linear and the magnitude of $2C_1$ was 1515 Pa, which was comparable to the shear modulus of the gels. Finally, the Tatara mechanical model was successfully used to extract the elastic modulus of the lens. This experimental technique will be used to determine the mechanical properties of the natural and prosthetic ocular lens.

Acknowledgements

This work was funded by a merit review grant to N.R. This work was also supported by awards to the Department of Ophthalmology and Visual Sciences from Research to Prevent Blindness, Inc. and the NIH (P30 EY 02687) Core grant.

References

[1] Park H, Park K. Hydrogels in bioapplications. In: Ottenbrite RM, Huang SJ, Park K, editors. Hydrogels and biodegradable polymers for bioapplications. Washington: American Chemical Society; 1996. p. 2–10.
[2] Griffith LG. Acta Mater 2000;48:263–77.
[3] Langer R, Vacanti JP. Science 1993;260:920–6.
[4] Peppas NA, Barr-Howell BD. Characterization of the cross-linked structure of hydrogels. In: Peppas N, editor. Hydrogels in medicine and pharmacy. Boca Raton, FL: CRC Press; 1987. p. 27–56.
[5] Torres-Lugo M, Peppas NA. Macromolecules 1999;32:6646–51.
[6] Fung YC. Biomechanics. 2nd ed. Mechanical properties of living tissues. New York: Springer; 1993.
[7] Fung YC. First course in continuum mechanics. 3rd ed. Upper Saddle River, NJ: Prentice Hall; 1993.
[8] Verdier C. J Theor Med 2003;5:67–91.
[9] Shanmugananda MK, Ravi N. Polym Prepr 1999;40:630–1.
[10] Murthy KS, Ravi N. Curr Eye Res 2001;22:384–93.
[11] Fisher RF, Hayes BP. QJ Exp Physiol 1982;67:213–24.
[12] Fisher RF. J Physiol 1969;201:1–19.
[13] Krag S, Andreassen TT. Exp Eye Res 1996;62:253–60.
[14] Krag S, Olsen T, Andreassen TT. Invest Ophthalmol Vis Sci 1997;38: 357–63.
[15] Kikkawa Y, Sato T. Exp Eye Res 1963;2:210–5.
[16] Ejiri M, Thompson HE, O'Neill WD. Vis Res 1969;19:233–44.
[17] Czygan G, Hartung C. Med Eng Phys 1996;18:345–9.
[18] Soergel F, Meyer C, Eckert C, Abele B, Pechhold W. J Refract Surg 1999; 15:714–6.
[19] Fetsch M, Hamilton P, Ravi N. Polym Mater Sci Eng 2003;44:285–6.
[20] Hertz H. J für die reine und angewandte Mathematik 1882;92:156.
[21] Tatara Y. J Eng Mater Tech 1991;113:285–91.
[22] Tatara Y, Shima S, Lucero JC. J Eng Mater Technol 1991;113:293–5.
[23] Mooney MJ. J Appl Phys 1940;1:582.
[24] Rivlin RS. Trans R Soc London, Ser A 1948;240:459.
[25] Tatara Y. J Soc Mech Eng Ser A 1993;36:190–6.
[26] Ellman GL. Arch Biochem Biophys 1959;82:70.
[27] Hansen JN, Pheiffer BH, Boehnert JA. Anal Biochem 1980;105:192–201.
[28] Hansen JN. Anal Biochem 1981;116:146–51.
[29] Hisano N, Morikawa N, Iwata H, Ikada Y. J Biomed Mater Res 1998;40: 115–23.
[30] Aliyar HA, Hamilton PD, Remsen EE, Ravi N. J Bioact Compat Polym 2005;20:169–81.
[31] Aliyar H, Hamilton PD, Ravi N. Polym Prepr 2004;45(2):366–7.
[32] Flory PJ, Rehner Jr J. J Chem Phys 1943;11:521–6.
[33] Peppas NA, Merrill EW. J Polym Sci, Part A: Polym Chem 1976;14: 459–63.
[34] Lee H, Park TG. Polym J 1998;(30):976–80.
[35] Ravi N, Mitra A, Hamilton P, Horkay F. J Polym Sci, Part B: Polym Phys 2002;40:2677–84.